

4-2013

## Application of the No-Core Symplectic Shell Model to Beryllium and Carbon Isotopes

Mia Cherise Ferriss

Follow this and additional works at: [https://repository.lsu.edu/honors\\_etd](https://repository.lsu.edu/honors_etd)



Part of the [Astrophysics and Astronomy Commons](#)

---

### Recommended Citation

Ferriss, Mia Cherise, "Application of the No-Core Symplectic Shell Model to Beryllium and Carbon Isotopes" (2013). *Honors Theses*. 501.

[https://repository.lsu.edu/honors\\_etd/501](https://repository.lsu.edu/honors_etd/501)

This Thesis is brought to you for free and open access by the Ogden Honors College at LSU Scholarly Repository. It has been accepted for inclusion in Honors Theses by an authorized administrator of LSU Scholarly Repository. For more information, please contact [ir@lsu.edu](mailto:ir@lsu.edu).

Application of the No-Core Symplectic Shell Model  
to Beryllium and Carbon Isotopes

by

Mia Cherise Ferriss

Undergraduate honors thesis under the direction of

Dr. Jerry P. Draayer &  
Dr. Kristina D. Launey

Department of Physics and Astronomy

Submitted to the LSU Honors College in partial fulfillment of  
the Upper Division Honors Program.

April, 2013

Louisiana State University  
& Agricultural and Mechanical College  
Baton Rouge, Louisiana

## Abstract

Using a schematic interaction that captures most of the physics of a realistic nuclear interaction and employing only a fraction of the ultra-large model space needed for conventional shell-model calculations, we explore collective and alpha-clustering substructures as part of a comprehensive study of light nuclei with number of particles ranging from 7 to 20. This is achieved by employing symmetries that dominate the nuclear dynamics. We show a successful application of the model that produces reasonable energy levels as well as additional physical observables. This improves our understanding of nuclear structure and could lead to further applications of the model, particularly to heavier and more complicated nuclei.

## Introduction

The goal of this research is to study the interaction within a nucleus and correlations inaccessible by other models. Consider beryllium-8, a nucleus of 4 protons and 4 neutrons. We consider this nucleus to be a cluster-structured nucleus. This means that this nucleus is composed of two alpha particles or helium-4 nuclei. Most often, Be-8 fission back into its constituent alpha particles. This almost instantaneous fission makes creation of heavier nuclei extremely difficult. Yet, within celestial bodies, when temperatures reach levels of 100 million K, helium may be converted into carbon-12, with the formation of Be-8 being a necessary step in this process. This process is known as the Triple Alpha Process. This is an immensely important step in element formation since C-12 is the basis of all organic life forms and without which we would not exist. This reaction starts a chain of nucleosynthesis, or construction of elements, which provides us with other, heavier elements that are necessary for life. Understanding the interactions that take place in alpha cluster-structured nuclei such as Be-8 and C-12 can lead to better understanding various stellar processes and to applications to other nuclei important in astrophysics. This study in particular, is the first to look at a comprehensive range of light nuclei.

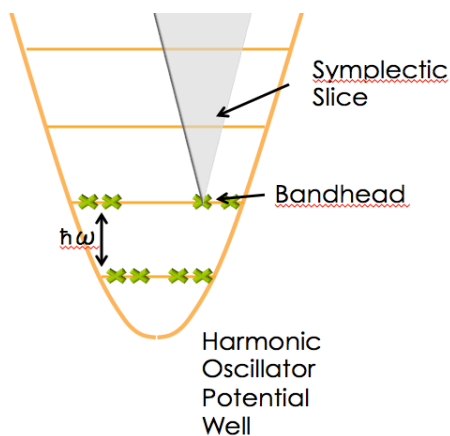


Illustration 1: Representation of the harmonic oscillator potential well with a bandhead and a symplectic slice. This example is a representation of Be-8.

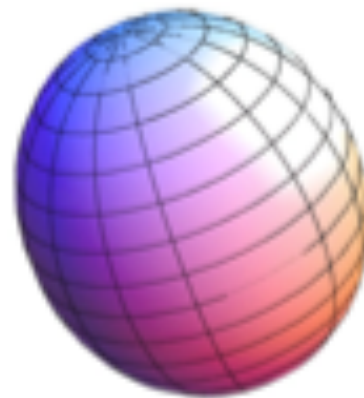


Illustration 2: Be-8's most deformed configuration, (4,0), for the particles shown in Illustration 1.

One successful approach to describing the structure of such atomic nuclei is the No-Core Shell Model, NCSM [1]. This model utilizes a realistic interaction (hence, it is referred to as “*ab initio*” or “from first principles”) and basis states that originate from the harmonic oscillator (HO) potential well. The model is considered no-core since each particle is active as opposed to being in a fixed core. It is a shell model due to the shells of the harmonic oscillator potential well, which is utilized due to it being a rough approximation of the interaction within a nucleus.

We use an adapted NCSM called the No-Core Symplectic Shell Model, NCSpM [3]. In the NCSpM we most often choose each nucleon to be in its lowest available state, filling as many shells as possible. This configuration is depicted in Illustration 1. There are many different configurations for these individual particles. We change our basis and instead of considering individual configurations of particles we use shape deformations since, due to an underlying symmetry, only a few shapes are typically dominant in the nucleus. This change of basis is just like a coordinate change from the x-y plane to cylindrical coordinates. This lowest configuration is what is referred to as a  $0\hbar\omega$  bandhead where  $\omega$  is the harmonic oscillator frequency and  $\hbar\omega$  is the energy release during a transition from level to level. On top of each bandhead we build a symplectic slice, which contains various deformations. These deformations are described with various quantum numbers. For example, the most deformed configuration of Be-8, which is shown in Illustration 2, is (4,0). This is a prolate or vertically stretched shape. We use a schematic interaction that captures the majority of the physics behind the nuclear interaction; and by utilizing the symmetries that dominate the nuclear dynamics we can use only a fraction of the model space necessary, but often not accessible, in conventional shell-model calculations [2].

Our model has been previously shown to reproduce reasonably well the energy levels and other physical observables (such as B(E2) transition strengths, radii, and quadrupole moments) of C-12, revealing the dominance of a clear, symplectic symmetry [3]. In the present comprehensive study, we explore clustering and alpha particle substructures to probe the success of the model further (without any adjustment to the parameters used in the C-12 study) for isotopes of Be with atomic masses ranging from 7 to 14 as well as isotopes of C with atomic masses ranging from 10 to 20. We again, as in the case of C-12, show reasonable reproductions of energy levels, transition strengths, rms (root-mean-squared) radii, and quadrupole moments. This is, in fact, a remarkable result given the simplicity of the interaction.

The one exception is Be-8, which, though it produces reasonable energy levels, reveals higher values for B(E2) transition strengths (indicative of collectivity) as compared to other theoretical predictions. In an effort to produce more reasonable B(E2) values without affecting accuracy in our energy levels, our interaction’s single parameter,  $\gamma$ , is systematically varied to describe this particular nucleus better. The particular alpha cluster structure of this nucleus or the fact that it is relatively light might contribute to the need for this adjustment.

Simply put, using the NCSpM, we explore collective and alpha-clustering substructures as part of a comprehensive study of light nuclei with masses ranging from 7 to 20. After this study, we can describe not only C-12 with our symplectic model, but also a wide range of nuclei and their isotopes. This could lead to the application of the model to heavier, more complicated nuclei, which could help us gain further insight into the features that dominate the nuclear structure.

## Theoretical Model

It is well-known that the schematic interaction,  $H=H_0 + \chi(Q \bullet Q)$ , works remarkably well in deformed nuclear systems (Bohr and Mottelson, Nobel Prize 1950), where  $H_0$  is the harmonic oscillator Hamiltonian and  $Q$  is the mass quadrupole moment. Indeed, the first order approximation of the long-range central nucleon-nucleon interaction is  $H_0$  and the second-order approximation is the quadrupole-quadrupole interaction ( $Q \bullet Q$ ).  $\chi$  is fixed by  $(\hbar\omega)/(\text{the number of excitations})$ , where the harmonic oscillator frequency  $\hbar\omega$  is determined by  $41/A^{1/3}$  for mass number  $A$ . Building on this successful schematic interaction, our interaction is  $H=H_0 + \chi/\gamma(e^{\gamma \frac{Q \bullet Q}{12}} - 1)$  [3]. Using the exponential allows us to take into account many-body interactions and imposes hierarchy. This is a crucial component when evaluating the advantages of our novel interaction as compared to the common one. Since the ( $Q \bullet Q$ ) interaction is extremely strong, if we were to excite two nucleons up twenty energy levels the common interaction would tell us that those nucleons would stay at that excited level. We know this to be incorrect since these particles seek to occupy the lowest energy levels. In essence, if we include multiple energy levels the common interaction fails. Since our model raises the ( $Q \bullet Q$ ) operator to the exponential we are in effect making this operator less and less important as particles become more and more excited. In our interaction the only added parameter is  $\gamma$ . The common interaction results for the limit in which  $\gamma \rightarrow 0$ .

Our interaction previously yielded good results for C-12, with  $\gamma = -0.00205$  [3]. With no other fitted parameters, we apply this interaction to beryllium and carbon isotopes. Our model space is divided into vertical symplectic slices starting with bandheads of  $0\hbar\omega$  (no excitations),  $2\hbar\omega$  (for example, 2 particles 1 HO shell up), and  $4\hbar\omega$  (as follows), and expanding above each bandhead up to  $N_{max} = 20$  (or  $20\hbar\omega$ ) – for comparison, current shell models reach up to about  $10\hbar\omega$ . These slices contain states that have a specific deformation. For each  $0\hbar\omega$ ,  $2\hbar\omega$ , or  $4\hbar\omega$  space, this study focuses on the collective rotation of the largest deformations, because they typically dominate in nuclei.

## Results and Discussion for Beryllium

### 1. Agreement with Carbon-12

A  $\gamma$  parameter of -0.00205 for C-12 previously yielded accurate results using our symplectic-based model [3]. With this C-12 data, we observed that our model was able to reproduce the first  $2^+$  and  $4^+$  states. In addition to these energy levels, this model was able to describe accurately the second  $0^+$  state, also known as the Hoyle state. This state is an excited state of C-12 that allows for the correct amount of C-12 to be created in stellar environments, beginning the chain of nucleosynthesis. Describing this state is a task that other *ab initio* models have not accomplished. The resulting energy spectrum is displayed in Figure 1. Without adjusting the  $\gamma$  parameter, we apply this interaction to Be-8. This model, as was the case with C-12, produces results of the same order for the energy spectrum of Be-8, calculates a value for the rms radius within the expected range, and again is able to calculate reasonably the second  $0^+$  state, a state not described by other *ab initio* models.

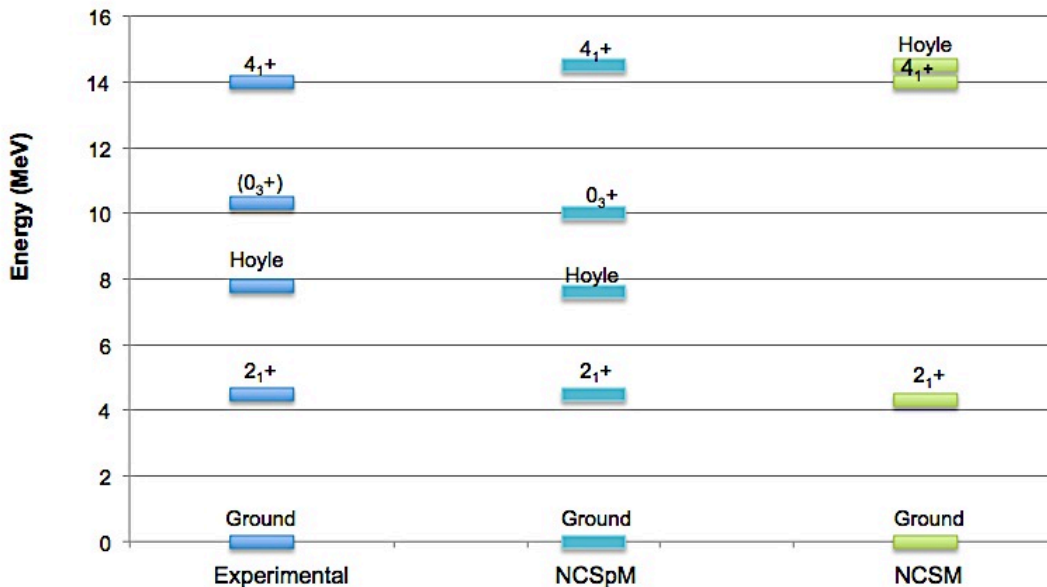


Figure 1. The experimental values [10], results from the NCSpM ( $N_{max} = 20$  and  $\hbar\omega = 18$  Mev), and the NCSM ( $N_{max} = 10$  and  $\hbar\omega = 15$  Mev) [4] are displayed here. All energies are in MeV. Figure reproduced from [3].

## 2. Be-8 Energy Spectrum

Calculations for the Be-8 spectrum include symplectic bandheads of the full  $0\hbar\omega$  space and are computed without adjustment of any parameters of the interaction, meaning  $\gamma$  for this spectrum is equal to -0.00205. All calculations were run with an  $N_{max} = 20$  and a  $\chi$  value of -30.0. This space is made up of deformations (4,0), (0,2), (1,0), and (2,1) together with the related symplectic excitations. The lowest levels,  $L = 0, 2, 4$ , of the most deformed  $2\hbar\omega$  and  $4\hbar\omega$  bandheads and their symplectic excitations are also included in this spectrum. Each of these bandheads has a deformation of (6,0) and (8,0), respectively. From (1,0), we have orbital momentum equal to 1 with a spin 1. In Figure 2, this state is labeled as a  $0^+$  to account for the lowest possible energy state that this

could represent. Deformation (2,1), in which orbital momentum is equal to 1, is also labeled  $0^+$  for similar reasons.

In the resulting energy spectrum displayed in Fig.2, there is good agreement with both the stretched symplectic model with Brink and Boekers interaction (Sp(1,R) with BB) [6] and experimental values, particularly for the (4,0) deformation, which describes the lowest  $0^+$ ,  $2^+$ , and  $4^+$  states. The Sp(1,R) model also uses a symplectic basis, but it considers a smaller model space than our NCSpM. According to our model, the first  $2^+$  state is calculated to be 4.40 MeV as compared to the Sp(1,R) model, which calculates the first  $2^+$  to be approximately 3.0 MeV [5]. These are both comparable to an experimental value of 3.03 MeV [10]. The other states belonging to the (4,0) deformation are of the correct order of magnitude according to experimental data. In addition, our results for the ground-state rotational band are found to lie very close to those of the *ab initio* calculations based on the Variational Monte Carlo (VMC) model and its extension, the Green Function Monte Carlo (GFMC) model [13] (see Table 1). These models employ realistic interactions and perform calculations in the coordinate space. However, our model yields a closer agreement to the experiment for the second  $0^+$  state as compared to the VMC energy prediction.

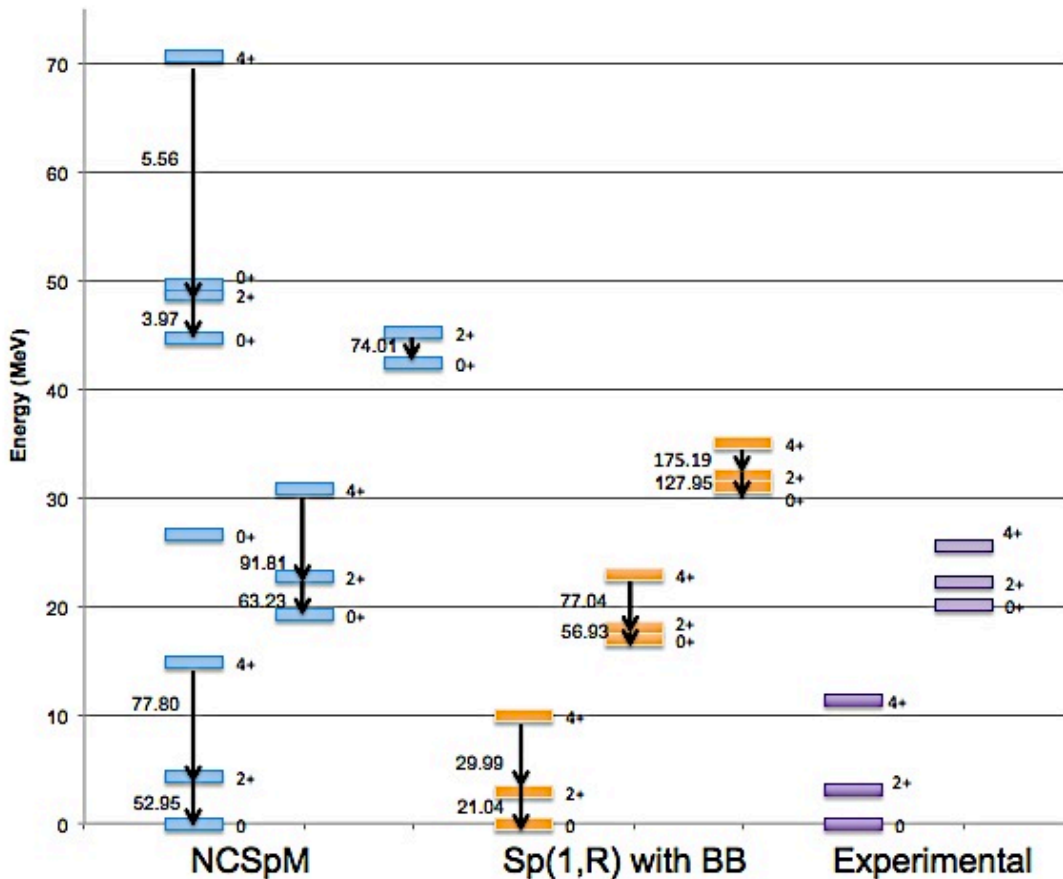


Figure 2. NCSpM and Sp(1,R) with Brink and Boekers (BB) interaction [6] compared to experimental values [10]. All energies levels are in MeV and all B(E2) transitions which are represented with the numbered arrows are in W.u. For each model, bandheads move from left to right starting with  $0\hbar\omega$  and moving to  $4\hbar\omega$ .

Although  $B(E2)$  values are not available for the experimental data, we are able to compare to the  $Sp(1,R)$  model [6], values of which are represented in Fig. 2 in W. u. units.  $B(E2)$  values for the lowest  $0^+$ ,  $2^+$  and  $4^+$  are rather high at this  $\gamma$  but of the same order as the values observed in the  $Sp(1,R)$  model. The ratio of the  $B(E2)$  values from  $4^+ \rightarrow 2^+$  to  $2^+ \rightarrow 0^+$  are nearly the same for the NCSpM and the  $Sp(1,R)$  model with ratios of 1.47 and 1.43, respectively.  $B(E2)$  values for both transitions from  $2^+ \rightarrow 0^+$  and  $4^+ \rightarrow 2^+$  are in closest agreement for the  $2\hbar\omega$  symplectic slice.

	VMC	GFMC	NCSpM	Exp.
Be-8( $2^+;0$ )	2.39(25)	2.91(25)	4.40	3.03(1)
Be-8( $4^+;0$ )	9.95(24)	9.58(27)	14.77	11.4(3)
Be-8( $0^+;0$ )	28.62(26)	N/A	19.28	20.2

Table 1. NCSpM and VMC/GFMC [13] energies and their errors for  $2^+$ ,  $4^+$ , and second  $0^+$  states (all with isospin  $T=0$ ) compared to experimental values. All energies are in MeV.

### 3. Other Beryllium Isotopes

The  $\gamma$  value of -0.00205 is also applied to other Be isotopes in order to compare calculated energy levels and  $B(E2)$  values with experimental values. The results are shown in Figure 3.

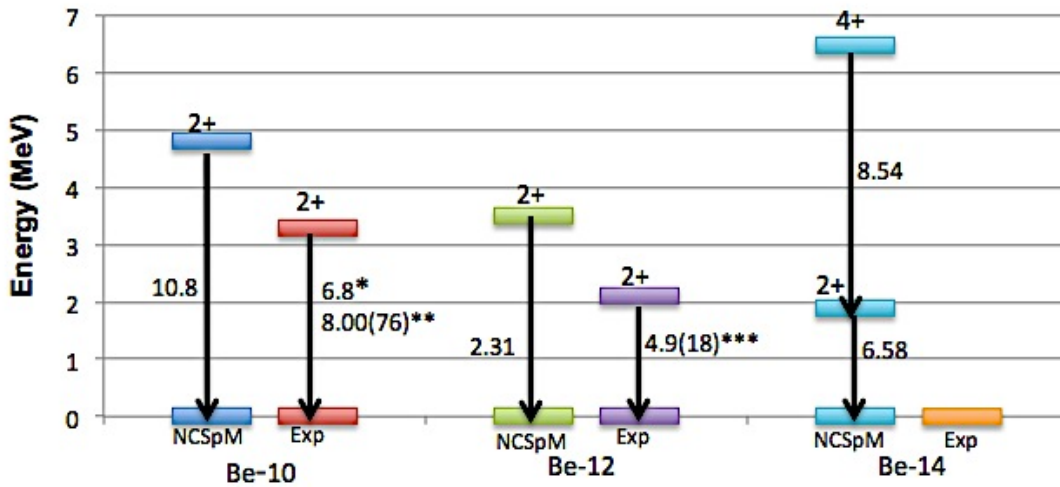


Figure 3. Be-10, Be-12, and Be-14 are represented here with values from our model on the left of each set of data for the isotope and experimental data displayed on the right. All energy levels are in MeV and all  $B(E2)$  values are measured in W.u. \* From reference [7]. \*\* From reference [10]. \*\*\*From reference [8].



In Figure 3, energy levels are displayed for Be-10, Be-12, and Be-14 [5]. Be isotopes for which we calculate B(E2) values, the rms radii, and quadrupole moments include Be-8 (4,0), Be-10 (2,2), Be-12 (2,0), and Be-14 (4,0). All were run with an  $N_{max}$  of 20, a  $\chi$  value of -30.0, -28.5, -27.0, and -25.5, respectively and an unadjusted  $\gamma$  equal to -0.00205.

For Be-10 and Be-12, the  $2^+$  states are each of the order of the experimental values. Also, the experimental values of the  $2^+$  states show a decreasing trend with the mass A, which is also reproduced in the NCSpM data. As for Be-14, a value for both the  $2^+$  and  $4^+$  states are calculated to be 1.9 MeV and 6.50 MeV, respectively [5]. In this case, there are no experimental values to which we can compare. This shows us that not only does the  $\gamma$  value for C-12 work without any adjusted parameters for Be-8, it also gives reasonable results for the energy spectrum of other Be isotopes without adjustment.

The reproduction of the energy levels produced by our model is remarkable but we must analyze agreement with other observable quantities such as B(E2), rms radii, and quadrupole moments, since they play an important role as well. In Figure 4, we have a plot of the B(E2) values for the various Be isotopes (also, see Fig. 3 for further representation of B(E2) values).

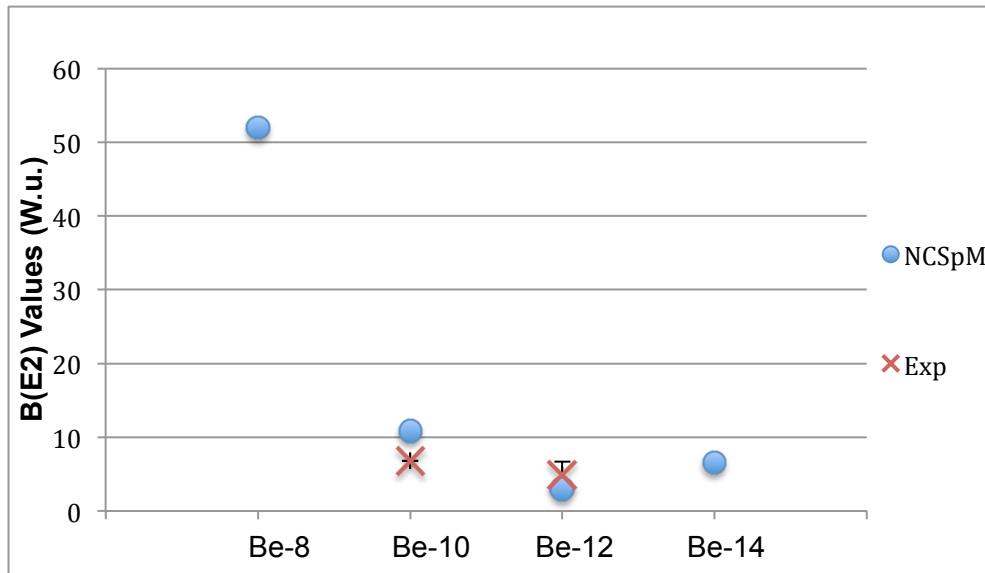


Figure 4. Even isotopes of beryllium ranging in atomic mass from 8-14 are displayed along the x-axis and each corresponding B(E2;  $2^+ \rightarrow 0^+$ ) value is measured in W.u.. Be-10 data from [7]. Be-12 data from [8].

While we have few experimental values for comparison, we do have reasonable estimations for both Be-10 and Be-12 with closer agreement for Be-12. For this isotope our calculation falls within error. B(E2) values are an indication of the collectivity of a particular nucleus with high B(E2) values indicating high collectivity. We can notice that for Be-8, our model yields an extremely large B(E2) value which speaks to its alpha-cluster structure. These alpha-cluster structures are extremely collective and our model demonstrates this. This is also an indication that the most deformed shape we use in our model does indeed dominate in these nuclei.

We are also able to compare experimental values to our calculated values of the rms radii for both even and odd isotopes of Be with the exception of Be-8. This lack of experimental data stems from this nucleus's short lifetime, making it impossible to measure its rms radius. Again, all isotopes were run with an  $N_{max}$  equal to 20. The bandhead deformations for the odd isotopes are chosen to be the most deformed, namely, Be-7 (3,0), Be-9 (3,1), and Be-11 (2,1).

The isotopes with atomic masses 9 through 12 show the best agreement, though Be-11 and Be-12 prove to be the most reasonable of the various isotopes. Note that this figure has an y-axis that begins at 2 fm, not 0, in order to more clearly display our data. With this in mind, when we refer to reasonable data points, we refer to a degree of reasonableness. When comparing our data points, our calculations for Be-12 show more reasonable agreement, specifically a 92% agreement, than Be-7, which shows a 77 % agreement. Be-14 has the highest experimental value at approximately 3.2 fm. While our calculations do not project a radius of quite this size, our projections do show an upward jump from Be-12 that falls within error. Our result for Be-7 shows the most disagreement with the experimental value. The experimental value indicates that this isotope is the most tightly bound, but our calculated value is in fact the least bound. This discrepancy may be due to shell effects that are not included in our model.

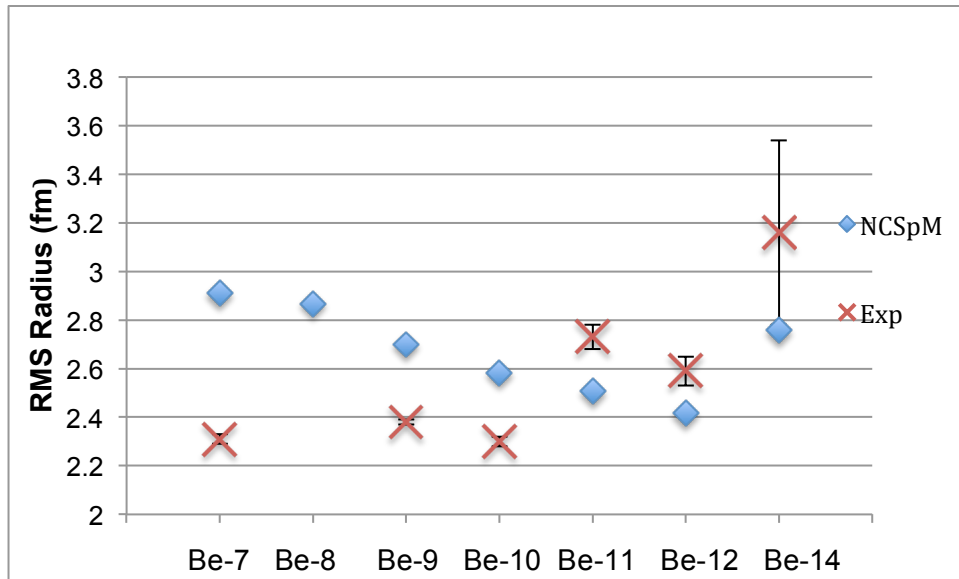


Figure 5. Each isotope of beryllium ranging from atomic mass 7 to 14 is represented with the exception of Be-13. Experimental data taken from [9]. Each ground-state radius is measured in fm.

Finally, we can also analyze the quadrupole moments for each of these nuclei. Again,  $N_{max}$  was equal to 20 and  $\gamma$  remained at  $-0.00205$ . While there are no experimental values for comparison, the results of our model are displayed in Figure 6. Given the good agreement for Be-10 and Be-12 for energies,  $B(E2)$  values and radii, we expect the quadrupole moment of these isotopes will be close to the ones predicted by the NCSpM. Agreement in all three observable

quantities again, supports the application of the model with a single  $\gamma$  value to C-12, Be-8, and other Be isotopes.

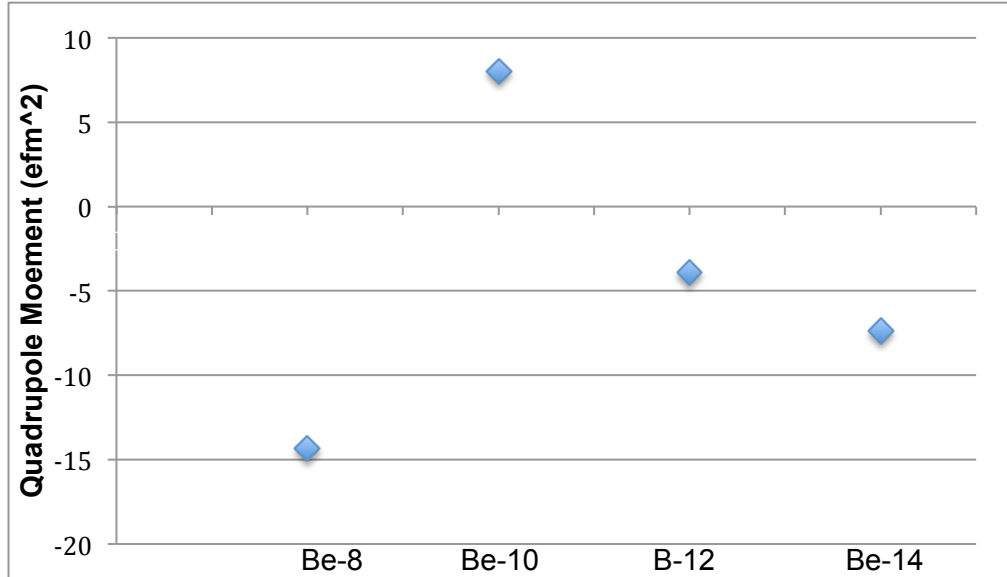


Figure 6. Isotopes are displayed along the x-axis and the corresponding quadrupole moments of the lowest  $2^+$  state are measured in  $\text{efm}^2$ .

## Results and Discussion for Carbon Isotopes

Just as our original  $\gamma$  of  $-0.00205$  is applied without adjustment to Be-8 and other isotopes, we expanded the original investigation of C-12 to other isotopes of C, namely all even isotopes spanning from atomic masses 10 to 20 without any parameter adjustment. We consider the most deformed states for each of these isotopes, which are as follows: C-10 (2,2), C-12 (0,4), C-14 (0,2), C-16 (4,2), C-18 (4,4) and (0,6), and C-20 (0,8). We consider two deformations for C-18 since, as Figures 7-11 will show, the most deformed (4,4) may not be the dominant deformation. We again use an  $N_{max}$  of 20 for each possible isotope with the exception of C-16 and C-18, which we reduce to an  $N_{max}$  of 16 due to matrix dimensions needed for eigenvalue calculations.  $N_{max} = 16$  appears to be sufficient since we can obtain convergence of results and still produce reliable values. The majority of the calculations are reported for angular momenta equal to 0 and 2, while C-12 and C-16 were run with angular momenta equal to 0, 2, and 4. Further calculations were done for C-12 in the original study and are displayed in several of the figures below.

## 1. Energy Levels of Various Carbon Isotopes

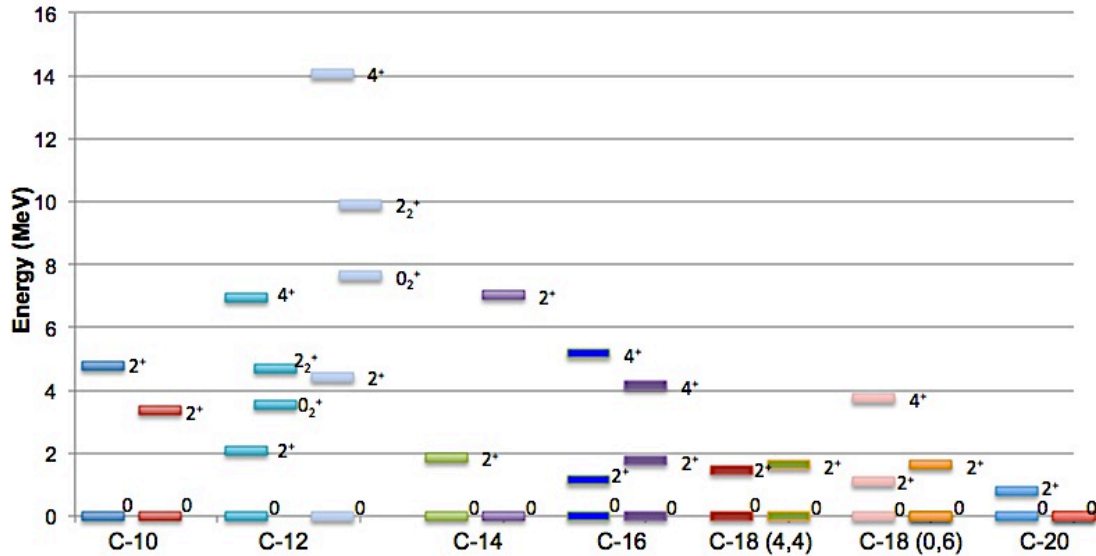


Figure 7. Even isotopes of carbon ranging in atomic mass from 10 to 20. On the left of each isotope is the NCSpM calculation and the right is experimental data [10]. C-18 is given for two deformations.

Our calculations of energy levels for C isotopes of the 2<sup>+</sup> states follow the general trend of the experimental energy levels. Starting at C-10, the 2<sup>+</sup> energy peaks at C-14 and then the energy levels lessen in magnitude as the atomic number increases. In all of the isotopes, with the exception of C-10, our spectrum is slightly compressed. For C-10 we calculate a value that is slightly above the experimental value of the first 2<sup>+</sup> state. C-12 may be scaled by a factor of 2 as done previously in order to produce more reasonable representations of each energy level [3], which would improve representations in C-14 as well, although with not as much reasonableness. C-14 is a particularly challenging nucleus due to its extremely long life-time. It is very likely that there are spin-orbit effects that are not within the scope of the model. The heavier nuclei, atomic masses 16 through 20, prove to be very reasonable without any scaling.

## 2. Observables for Carbon Isotopes

In Figure 8, we display the B(E2) values for various C isotopes from their 2<sup>+</sup> states to the ground states. The NCSpM data are compared to both experimental data and theoretical data that were produced by extrapolating NCSM results [11]. Again, both deformations of C-18 are represented. Here (4,4) produces a B(E2) value of 3.95 W.u. while (0,6) produces a value of 2.73 W.u. This is the first instance we have encountered in which the most deformed configuration (4,4)

may not dominate within a nucleus, at least when considering  $B(E2)$  values. We have good agreement for most of the C isotopes with the exception of C-10 and C-16. For C-10, our symplectic model produces a  $B(E2)$  value of 24.46 W.u. as compared to an experimental value of 6.88 W.u. [11]. Another, closely lying  $2^+$  yields a NCSpM value of only 4.64 W.u. This discrepancy could be due to significant mixing within the nucleus. Also, we calculate a value of 6.26 W.u. as compared to a value of 1.08 W.u. for C-16 [4]. Other than these two discrepancies, we can observe a general trend of decreasing  $B(E2)$  values beginning with C-10 and reaching a low point at C-16 and then increasing for C-18 and C-20. This follows the trend in experimental  $B(E2)$  values and the NCSM-extrapolated results.

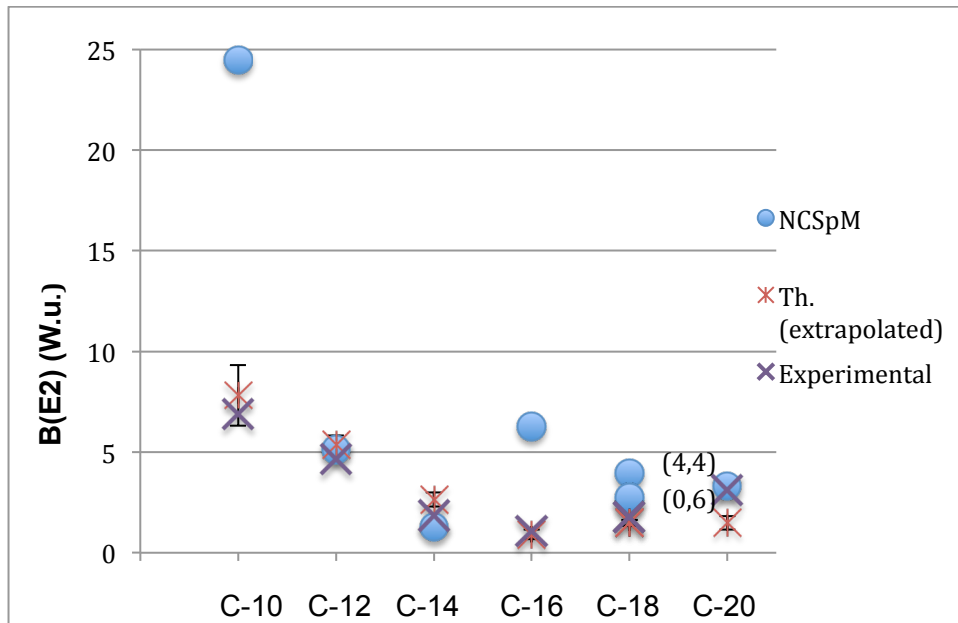


Figure 8. NCSpM values for the  $B(E2; 2^+ \rightarrow 0^+)$  values are compared to both experimental values [10] as well as theoretical values calculated by Forssen *et al.* [11] by extrapolating *ab initio* NCSM results.

In Figure 9, we show a comparison of our calculations to experimental values for the rms radii for various C isotopes. While there is no comparison for C-10, we are able to look at the other isotopes. The NCSpM calculations again follow the general trend of the experimental data with C-16 proving to be the most reasonable. For C-18, we again consider two deformations, both (4,4) and (0,6) but it is the most deformed, (4,4), that more closely matches the radius measurement as expected.

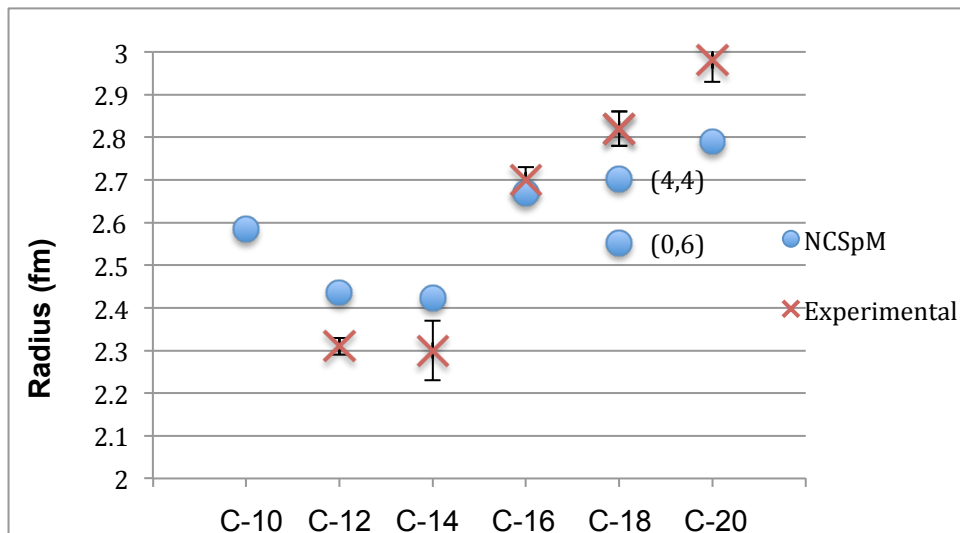


Figure 9. NCSpM calculations for the ground-state rms radii are compared to experimental data quoted from [12]. Each radius is measured in fm.

Finally, we can compare the quadrupole moment for each isotope. We observe extremely reasonable results for many of the nuclei, particularly C-12 and C-14. There are two discrepancies present: one in the quadrupole moment of C-10, for which we calculate a moment of opposite sign, and second in C-16, for which we have sign agreement but disagreement in magnitude. These are the same two isotopes of carbon for which there were discrepancies in the  $B(E2)$  values. In fact, for C-10 the other  $2^+$  state yields a negative, but large, quadrupole moment of  $-11.63 \text{ efm}^2$ . This again points to significant mixing of these  $2^+$  states in this nucleus and may suggest a difference in the underlying structure. Again, in these calculations of the quadrupole moment, the most deformed representation of C-18 (4,4) does not reproduce even the correct sign. Instead (6,0) produces a very reasonable value as compared to the extrapolated fit.

Now, with the application of  $\gamma$  to isotopes of C other than C-12, we can see this is an extremely reasonable value for our parameter. Not only do we see close reproductions of the majority of energy levels, we observe reasonable values for physical observables such as  $B(E2)$  values and rms radii with only a few exceptions.

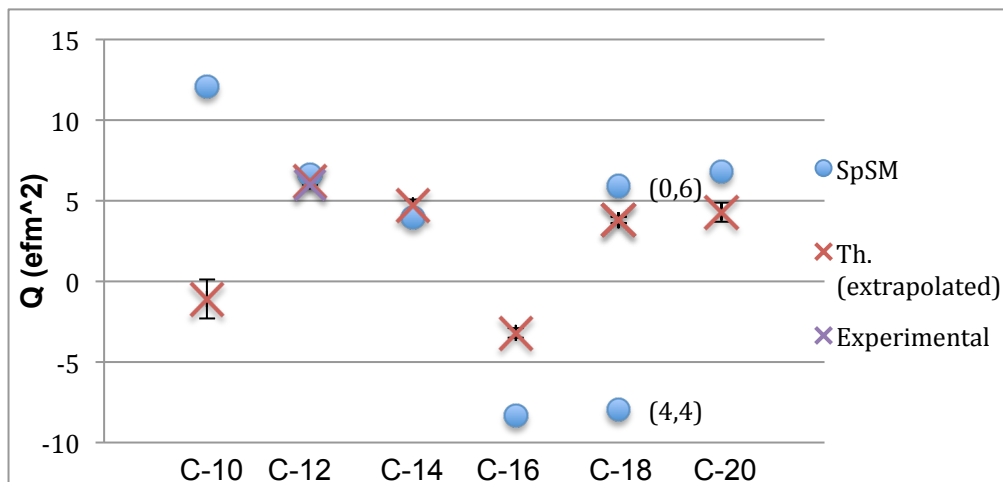


Figure 10. NCSpM values for the theoretical quadrupole moment of the lowest  $2^+$  state are compared to experimental data quoted from [11] as well as to theoretical values calculated by Forssen *et al.* [11] by extrapolating *ab initio* NCSM results.

## Results and Discussion for Adjusting the $\gamma$ Value

### 1. Role of $\gamma$ for Be-8

Recall from Figure 2 that while we had reasonable representations for the energy levels of Be-8, our  $B(E2)$  transition values were relatively high. This discrepancy allows us to utilize the parameter in our interaction and see its effect on transition strengths for nuclei of different atomic masses and the alpha clustered structures, Be-8 in particular. To study this effect we performed several  $\gamma$  spans.

Here, we have the  $\gamma$  span ranging from  $\gamma = -0.0001$  to  $-0.1$ . This  $\gamma$  span was run for the entire  $0\hbar\omega$  space as well as the  $2\hbar\omega$  and  $4\hbar\omega$  bandheads and the symplectic excitations on top up to  $N_{max} = 20$  of Be-8 [5]. The value of  $\gamma$  is incremented in such a way that it steps down a tenth for each calculation with all other parameters remaining the same. Also, both states in which  $L=1$  and spin=1 from the (1,0) and (2,1) deformations are labeled as a  $0^+$  state.

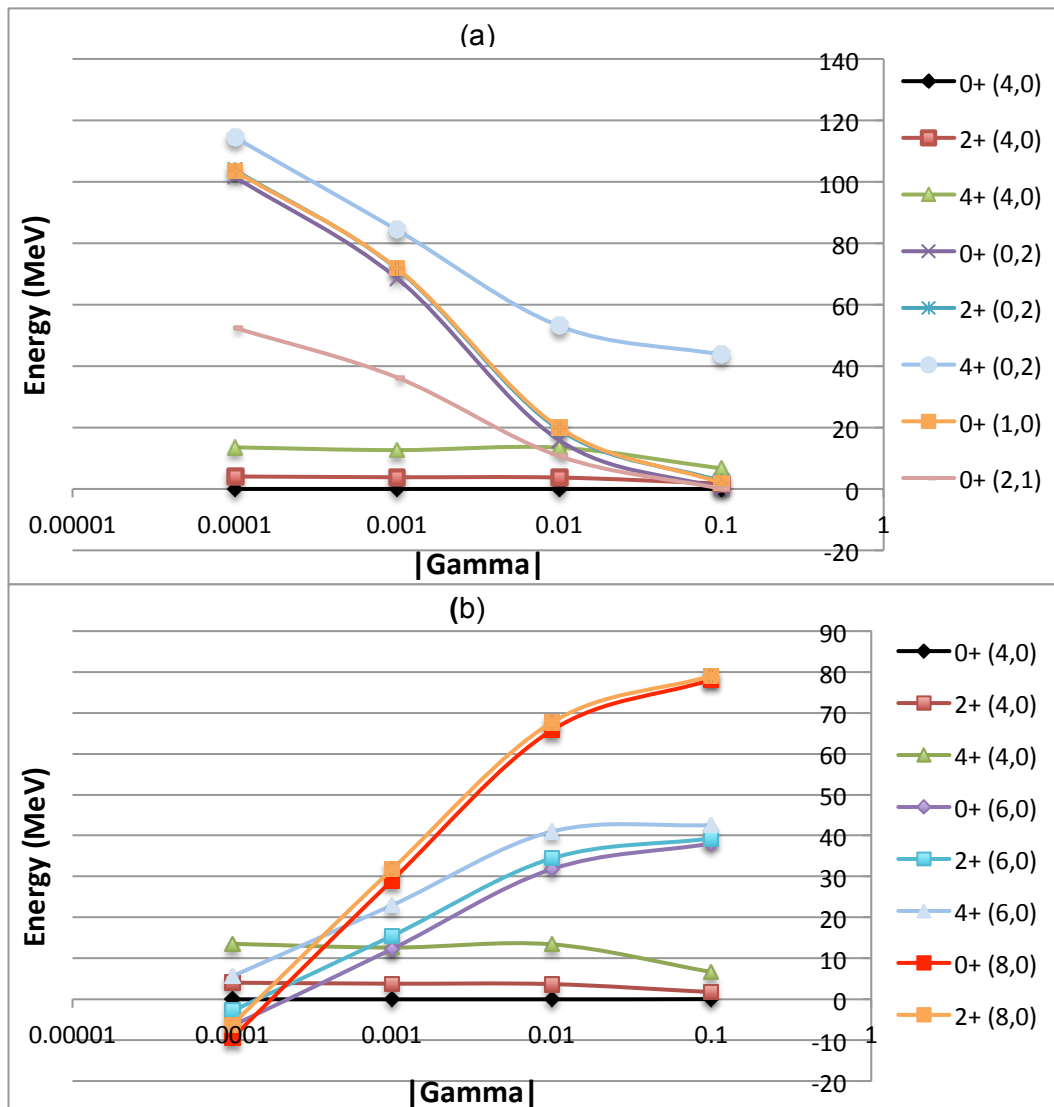


Figure 11. All energies are measured in MeV along the y-axis with each  $\gamma$  value represented on the x-axis. Each series of data is represented by its bandhead deformations as seen in the legend. (a) all symplectic slices that start at  $0\hbar\omega$ . (b)  $0\hbar\omega$  (4,0) that describes the ground state rotational band together with  $2\hbar\omega$  (6,0) and  $4\hbar\omega$  (8,0) that describe low-lying  $0^+$  states.

Correct ordering of the states occurs between  $\gamma = -0.001$  and  $-0.01$  (Fig.11). We can see that states of (4,0) lie lowest within this range. We can also observe the drastic dependence of both the  $2\hbar\omega$  and  $4\hbar\omega$  (Fig.11 b) on the  $\gamma$  parameter with both excitations becoming increasingly large as  $\gamma$  decreases. Note that the  $0^+$  from both (1,0) and (2,1) lie on top of one another for the entire  $\gamma$  span. Figure 11 also suggests that correct ordering would occur with a  $\gamma$  slightly closer to  $-0.001$  than  $-0.01$ , which again supports the choice of  $\gamma=-0.00205$ .

While we do calculate extremely reasonable energy levels for the  $0\hbar\omega$ ,  $2\hbar\omega$ , and  $4\hbar\omega$  space, the  $B(E2)$  values, which are indicative of collectivity, were relatively high for each transition, particularly for the lowest-lying energy levels in the (4,0) deformation, which include the ground state, the first  $2^+$ , and the first  $4^+$  states. In order to decrease the magnitude and improve the reasonableness of these values, the  $\gamma$  span is narrowed beginning with the values  $-0.001$  and  $-0.01$ , which, as shown in Fig. 11, contains the correct ordering of energy levels and does not render the wavefunction unphysical. We performed a systematic division of this range in order to compare the energy spectrum and  $B(E2)$  values produced by different  $\gamma$ . The  $\gamma$  span led us to focus on a  $\gamma$  value of  $-0.00365$ . The energy spectrum produced by this  $\gamma$  value is displayed in Fig. 12. The energies of the ground-state rotational band ( $0^+$ ,  $2^+$ , and  $4^+$ ) agree with the corresponding *ab initio* results derived in the framework of GFMC [13] and NCSM [14].

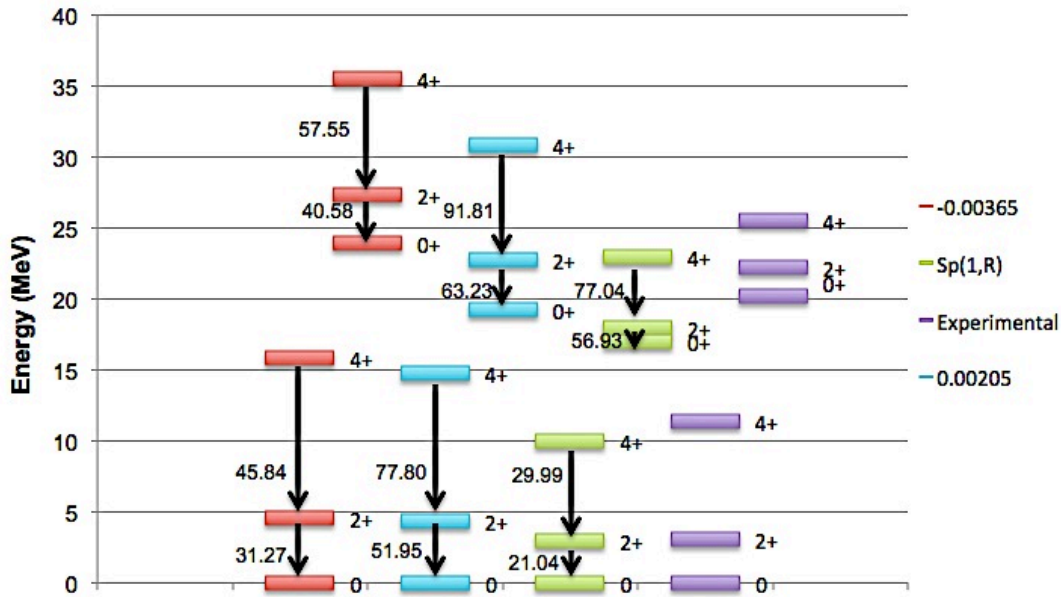


Figure 12. NCSpM and Sp(1,R) with Brink and Boekers interaction [6] compared to experimental values. All energies are in MeV and all  $B(E2)$  transitions are in W.u.



## 2. RMS Radius for Various Beryllium Isotopes

To study the effect of  $\gamma$ , we performed calculations for the rms radius for isotopes of even atomic masses. These included Be-8, Be-10, Be-12 and Be-14. Each isotope was run for an  $N_{max}$  equal to 20, with their respective  $\chi$  values equaling -30.0, -28.5, -27.0, and -25.5, and for angular momenta,  $L=0, 2, 4$  [5]. Within each run, an rms radius value is calculated for various  $\gamma$  values ranging from  $\gamma = -0.1$  to  $-0.0001$ , the exception being Be-14, which was only run for  $\gamma = -0.01$  and  $-0.00205$ . The  $\gamma$  value is incremented in such a way that it steps down a tenth for each calculation with all other parameters remaining the same. The exception is  $\gamma = -0.00205$  [5]. This is the  $\gamma$  value from earlier calculations for C-12. This  $\gamma$  was also run with an  $N_{max}$  equal to 20 and angular momenta  $L=0, 2, 4$  [5]. The results are displayed in Figure 13.

As mentioned before, Figure 13 contains only calculated values for Be-8, Be-10, Be-12, and Be-14. Odd isotopes are included in this figure since both experimental values and values from the fermion molecular dynamic (FMD) model are both available [9]. Inclusion of these odd isotopes allows us to observe the relationship between the rms radius and atomic mass for each Be isotope.

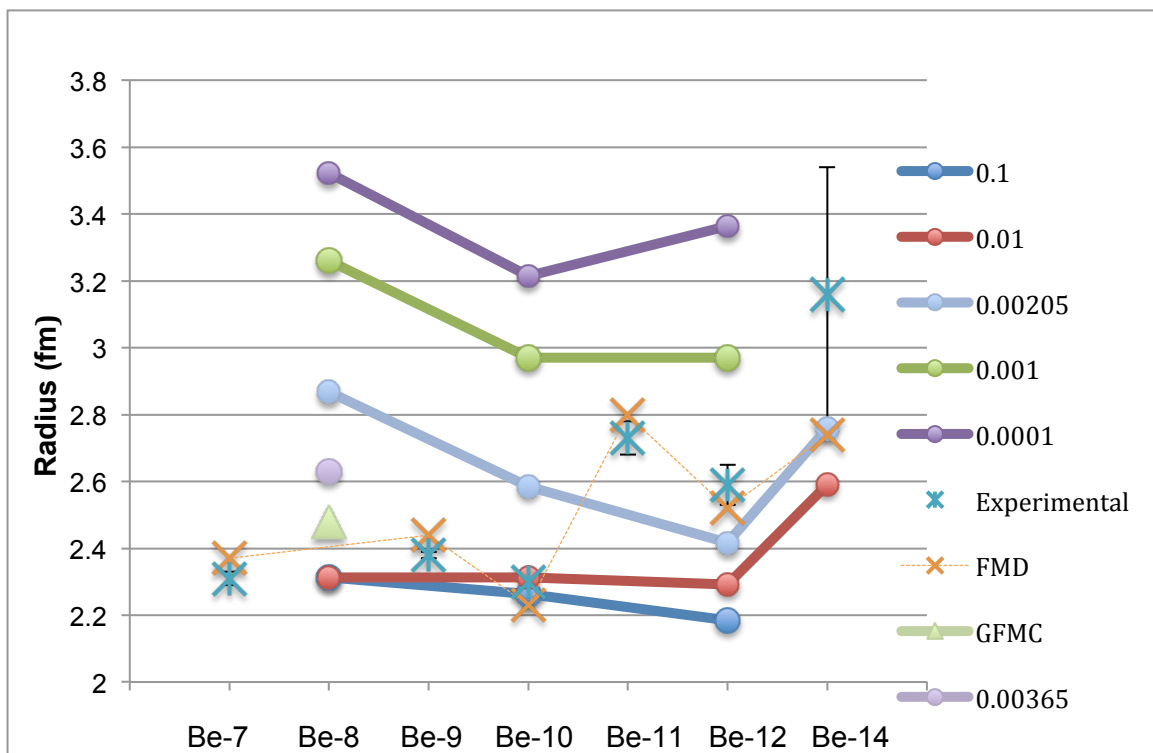


Figure 13. Each isotope is displayed along the x-axis with the corresponding ground-state rms radius for each gamma or model measured in fm. Theoretical FMD and experimental values are from [9] and theoretical VMC/GFMC from [12].

The FMD model and experimental data's shape closely follow each other until the Be-14 isotope is reached. This provides us with a reasonable range within which the Be-8 rms radius could fall. By first examining the data for  $\gamma = -0.0001$  we can see that this  $\gamma$  range affects the radius in such a way that it falls out of any range that agrees with previous models. We can then step down and look at  $\gamma = -0.001$  and see that this  $\gamma$  more closely follows the expected path for each isotope, but predicts a high value, near 3.2 fm, for Be-8. Stepping down yet again we observe that both  $\gamma = -0.1$  and  $-0.01$  closely follow the experimental and FMD model, and giving a relatively low value for the rms radius of Be-8. The value of  $\gamma = -0.01$ , in particular, produces accurate values for both Be-10 and Be-14. While  $\gamma = -0.01$  calculates close values for both lower and heavier atomic masses,  $\gamma = -0.1$  remains low for heavier isotopes. We can also see  $-0.00365$  falls closer to the value estimated by the GFMC model than  $-0.00205$  making this a viable candidate for an adjusted  $\gamma$  considering Be-8's cluster structure. A value of  $\gamma = -0.00365$  produces a rms radius of 2.63 fm, which is very close to the GFMC value of 2.48 fm.

### 3. Observables for Beryllium Isotopes for an Improved $\gamma$ Value

In Figure 14, we have the B(E2) values for various Be isotopes with even atomic masses. These values are calculated using a  $\gamma$  of  $-0.00365$ . Experimental data is scarce for the B(E2) values of Be isotopes, but we were able to obtain two experimental values from different studies. We have excellent agreement for both Be-10 and Be-12. Our calculated values for these isotopes are 10.8 and 2.3 W.u., respectively, and the experimental values are estimated to be 6.8 W.u. [7] and 4.9(18) W.u. [8].

A chi-squared test was performed to analyze the difference between the B(E2) values with a  $\gamma$  equal to  $-0.00205$  as compared to a  $\gamma$  equal to  $-0.00365$ . For  $\gamma = -0.00205$ , the chi value is 1.7991 and for  $\gamma = -0.00365$ , the chi value is 1.5455. This represents nearly a 15% improvement in accuracy of B(E2) values for  $\gamma = -0.00365$ .

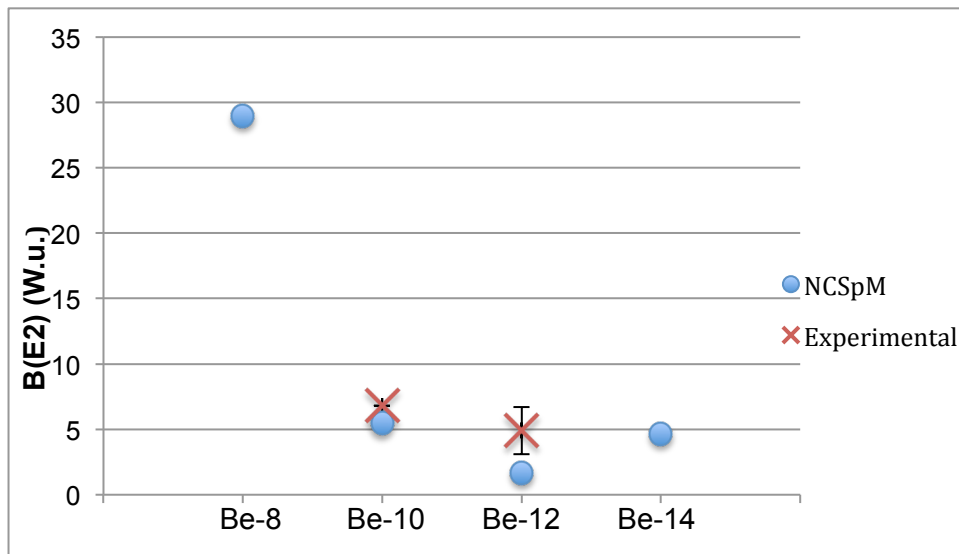


Figure 14. Even isotopes of Be ranging in atomic mass from 8-14 are displayed along the x-axis and each corresponding B(E2;  $2^+ \rightarrow 0^+$ ) value is measured in W.u. Be-10 data from [7]. Be-12 data from [8].

In Figure 15, we have a comparison of the rms radii for various Be isotopes. We calculate both odd and even isotopes for comparison, with the exception of Be-13. As previously mentioned, the only value we are not able to quote for comparison is the radius for Be-8, which is due to its extremely short half-life, making it impossible to obtain an experimental value for this isotope. The calculations for each other isotope generally follow the trend of the experimental data. Be-9 and Be-10 show particularly good agreement with calculated values as compared to experimental.

A chi-squared test was also performed for the rms radius to compare our two values for  $\gamma$ . For  $\gamma$  equal to -0.00205, the chi value is 0.5597. For the  $\gamma$  equal to -0.00365, the chi value is 0.4181. This represents a 25% difference in favor of the  $\gamma$  equal to -0.00365, suggesting that it represents the more accurate description of the rms radius of various Be isotopes.

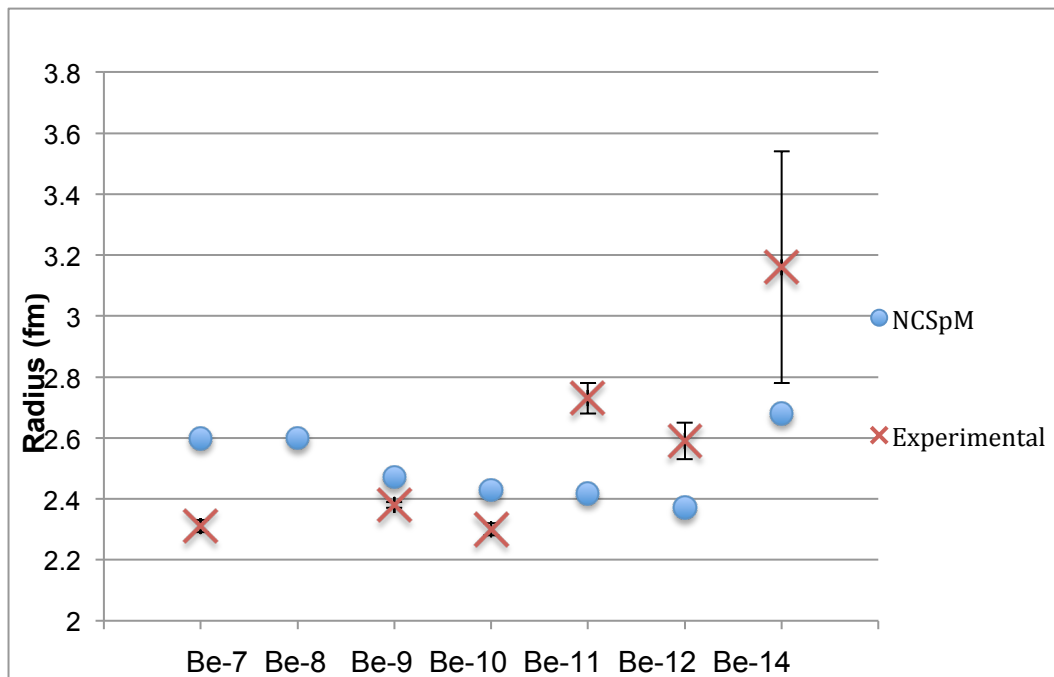


Figure 15. The ground-state rms radii for various Be isotopes is shown above. Each isotope of Be ranging from atomic mass 7 to 14 is represented with the exception of Be-13 with each corresponding radius measured in fm. Experimental values are quoted from [9].

The largest discrepancies occur at the lightest isotope, Be-7. Our calculations suggest that Be-7 is one of the least tightly bound isotopes while experimental data shows it is actually one of the most tightly bound. This  $\gamma$  value of -0.00365 also calculates a reasonable prediction for Be-8, as before, with a radius measuring 2.6 fm.

In Figure 16, we show the quadrupole moments for various isotopes of Be calculated using a  $\gamma$  of -0.00365. There is no available experimental data for comparison, so this figure displays only the calculations from our model. Due to good agreement in other observables (BE(2) values and rms radii) for Be-10 and Be-12 we expect the quadrupole moment of these isotopes to be near the actual values. Figure 16 also illustrates the evolution of the ground-state deformations

with A. Be-8 is strongly prolate with two alpha particle aligned next to each other, while Be-10 has an oblate shape. After Be-10 as the isotopes become richer in neutrons they become more prolate shaped.

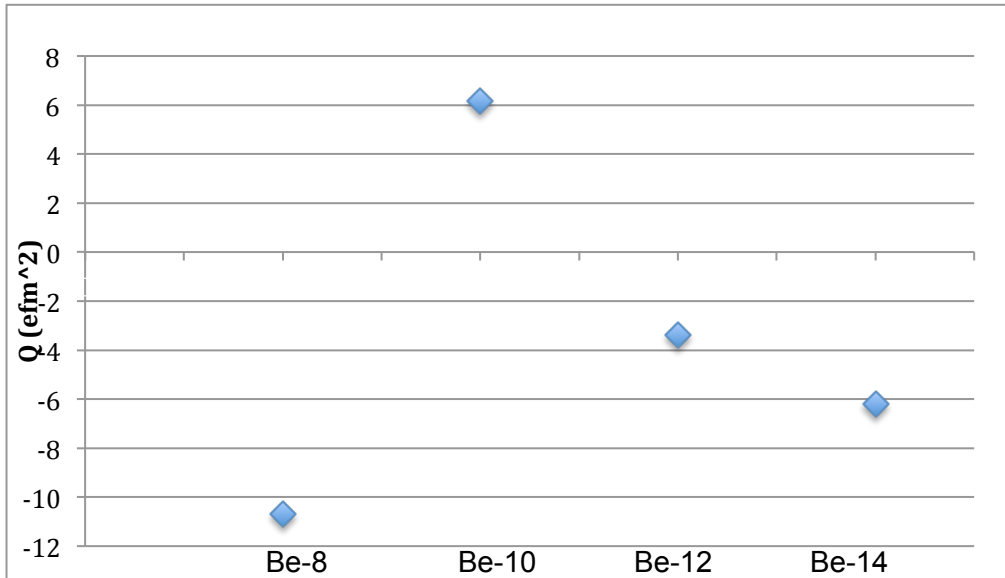


Figure 16. The quadrupole moment of the lowest  $2^+$  state for various isotopes is shown above. Isotopes are displayed along the x-axis and the corresponding quadrupole moments are measured in  $\text{efm}^2$ .

By varying  $\gamma$  in a systematic way, we have been able to achieve a reasonable description of Be-8 and its properties. For this cluster-structured nucleus, this variation of  $\gamma$  allows us to adjust our calculations when the structure of a particular nucleus is cluster driven. With this adjustment, other observables remain reasonable and we even see, through chi-squared calculations, improvements in the  $B(E2)$  values and rms radii of other Be isotopes.

## Summary

This study showed that the symplectic symmetry-based NCSpM model yields remarkably good results for several properties of beryllium isotopes with  $A = 7$  through 14 and carbon isotopes with  $A = 10$  through 20 without any adjusted parameters from the previously successful study of C-12. These properties included energy spectra,  $B(E2)$  transition strengths, rms radii, and quadrupole moments. The close agreement with the experiment for this wide range of isotopes is a significant result further confirming the importance of the simple interaction we used and the symmetry-based selection of the model space. In addition, we were able to account for excitations up to  $N_{max}=20$ , which is much beyond the conventional shell model reach and which proved essential to achieve reasonable descriptions. We also studied the effect of our model parameter on each of these isotopes and were able to systematically vary this parameter in order to achieve more reasonable agreement with physical

observables for alpha-cluster driven structures such as Be-8. The model provided estimates for various observables that are not currently available from experiment, as well as valuable information on the shape deformation of proton- to neutron-rich Be and C isotopes.

This is the first systematic study of light nuclei using NCSpM that shows reasonable agreement in not only C-12, but also a wide range of nuclear isotopes. This could lead to the application of the NCSpM to heavier, more complicated nuclei, and inform us about their dominant features.

## References

- [1] P. Navratil, J. P. Vary, and B. R. Barrett, "Properties of  $^{12}\text{C}$  in the Ab Initio Nuclear Shell Model". *Phys. Rev. Lett.* 84, 5728 (2000)
- [2] T. Dytrych, K. D. Sviratcheva, C. Bahri, and J. P. Draayer, "Dominant role of symplectic symmetry in ab initio no-core shell model results for light nuclei". *Phys. Rev. C* 76, 014315 (2007)
- [3] A. Dreyfuss, K.D. Launey, C. Bahri, T. Dytrych J. P. Draayer, "Microscopic description of the elusive Hoyle state". APS Conference, DNP, Michigan State University (2011)
- [4] P. Maris and J. P. Vary, private communication (2012)
- [5] M. Ferriss, G. Tobin, K. D. Launey, T. Dytrych, J. P. Draayer, "Symmetry-guided description of light nuclei with schematic and realistic interactions", to be submitted (2013)
- [6] F. Arick *et al*, "*The  $Sp(2,R)$  Model Applied to Be-8*". *Nucl. Phys. A* 318, 269 (1979)
- [7] E. A. McCutchan, C.J. Lister, private communication (2008)
- [8] Imai *et al.*, "First lifetime measurement of  $2^+_1$  state in Be-12". *Phys. Lett. B* 672, 179 (2009)
- [9] A. Krieger, "Nuclear charge radius of  $^{12}\text{Be}$ ". arXiv:1202.4873 (2012)
- [10] National Institute of Standards and Technology, NIST, <http://www.nist.gov/index.html>
- [11] C. Forssen, R. Roth, P. Navratil, private communication (2012)
- [12] A. Ozawa, "Measurements of interaction cross sections for light neutron-rich nuclei at relativistic energies and determination of effective matter radii". *Nucl. Phys. A* 691, 599–617 (2001)
- [13] R. B. Wiringa, S. C. Pieper, J. Carlson, and V.R. Pandharipande, "Quantum Monte Carlo calculations of  $A=8$  nuclei". *Phys. Rev. C* 62, 014001 (2000)
- [14] P. Maris, J. P. Vary, and P. Navratil, "Structure of  $A = 7-8$  nuclei with two-plus three-nucleon interactions from chiral effective field theory". *Phys. Rev. C* 87, 014327 (2013)